been proposed[18b,37] that a better description of the conductive form of PA is as an open shell cation radical species, rather than as a protonated imine (see Scheme I). Our work does not speak to the proper description of the conductive form of PA, but rather it addresses the stoichiometry of the electron and proton transfers associated with the various oxidation and reduction steps. We show the conductive form as consisting of a mixed amine/protonated imine structure simply as a way to indicate partial oxidation, not to imply support for one structure over another.

Further quantitative comparisons of our data with those of others are possible from the work of Gottesfeld et al.,[39] who recently studied the ellipsometric behavior of PA films. Among other things they were able to measure the film thickness and determine a correlation between the anodic charge consumption (our Q_{ox}) and the thickness. Assuming a film density of 1.2 g/cm^3 to calculate the thickness from Γ_{PA}, our results agree quantitatively (to within 5%) with theirs. Thus, measurements probing widely different properties using completely different techniques give excellent agreement, lending strong support to the quantitative aspects of both techniques.

Wrighton and co-workers have published a detailed study of the dependence of the resistance of PA on electrode potential.[2] They show that the resistance begins to drop at the very initial stages of the first oxidation process, when less than 10% of the oxidative charge has been passed. Our results show that significant charge is passed before the insertion of anions during the first oxidation process in 1 M acid which can be interpreted as meaning that deprotonation of the film to reach the conductive form shown in Scheme I, followed by proton loss to the external solution, occurs immediately on initiation of this oxidation process. These two results taken together argue that in acid solutions in which the reduced form is significantly protonated, formation of the resonance stabilized conductive form by deprotonation is a prerequisite for conductivity and that a small amount of oxidation induces deprotonation which can lead to large changes in conductivity.

The finding that protons can have a significant role in the charge compensation process for PA is germane to its possible use as a battery material. To the extent that protons take part in this process, the energy density of the battery will be improved. In addition, it is not unreasonable to suppose that proton transport should be faster than anion transport, so that larger power densities could be achieved. We are currently examining the rates of the switching process in various media in which the charge compensating ions are known to be predominantly anions or protons so as to probe these questions further.

A major result of this work is the demonstration that by providing additional constraints on models for experimental systems, the QCM can provide a wealth of information on electrochemical processes that involve mass changes of the electrode surface. This is especially true for thin films on electrode surfaces in which solvent and ion transport processes are very difficult to quantify by other methods. We are currently examining several other thin film systems such as polythiophene, polypyrrole, and polyvinylferrocene to determine the importance of these processes to the kinetics and thermodynamics of their electrochemical reactions. As the technique develops and its sensitivity is improved, we expect that even monolayer adsorption of organic species will be measurable. In fact, it has already proved possible to monitor monolayer adsorption/desorption of surfactants derivatized with redox groups.[40] We feel that because of its relative ease of use and low cost the QCM should become a widely used technique for probing electrochemical surface processes.

Acknowledgment. This work was supported by a grant from Research Corp. Additional financial assistance was provided by the University of Wyoming, Division of Basic Research. Many enlightening discussions with Professor Ed Clennan are gratefully acknowledged.

Registry No. PA, 25233-30-1; HCl, 7647-01-0; HBr, 10035-10-6; H_2SO_4, 7664-93-9; $HClO_4$, 7601-90-3; CF_3CO_2H, 76-05-1.

(40) Donohue, J.; Buttry, D. A., manuscript in preparation.

Photoassisted Catalytic Dissociation of H_2O To Produce Hydrogen on Partially Reduced α-Fe_2O_3

M. M. Khader, G. H. Vurens,† I.-K. Kim, M. Salmeron,† and G. A. Somorjai*

Contribution from the Materials and Molecular Research Division, Center for Advanced Materials, Lawrence Berkeley Laboratory and Department of Chemistry, University of California, Berkeley, Berkeley, California 94720. *Received October 30, 1986*

Abstract: The photodissociation of H_2O on partially reduced Fe_2O_3 powders and pellets is shown to be a catalytic process if the semiconductor is illuminated by visible light of energy greater than 2.2 eV. Activation of the Fe_2O_3 catalysts involved reduction in a mixture of H_2 and H_2O followed by oxidation. Up to 380 μmol of H_2 were produced with 190 μmol of Fe_2O_3 powder. The rate was 40 μmol h^{-1} g^{-1} for the first 200 h and started to decay thereafter. O_2 was also produced as shown by using $H_2{}^{18}O$ in amounts of up to 40 ± 15% of the amount of H_2 detected in the same experiment. In photoelectrochemical experiments with use of a three compartment cell the active pellets produced photocurrents of approximately 4 μA cm^{-2} mW^{-1} at +0.5 V bias (SCE, pH 13). Simultaneously, H_2 was produced at a rate of 0.06 μmol h^{-1} mW^{-1}. A lower limit to the conversion efficiency of approximately 10^{-3} H_2 molecules per photon is obtained.

Iron oxide has been investigated extensively in recent years to probe its ability to dissociate water either by photoassisted electrolysis[1-11] or by a photocatalytic reaction.[12] It has also been recently reported as an active catalyst in producing NH_3 from N_2 and H_2O.[13,14] The material is an n-type semiconductor with an indirect band gap of 2.2 eV.[15] The excitation of photoelectrons from the valence band to the conduction band requires visible light,

* Department of Chemistry.
† Center for Advanced Materials.

(1) Hardee, K. L.; Bard, A. J. *J. Electrochem. Soc.* **1976**, *123*, 1024; **1977**, *124*, 215.
(2) Curran, J. S.; Gissler, W. *J. Electrochem. Soc.* **1979**, *126*, 56.
(3) Yeh, L. R.; Hackerman, N. *J. Electrochem. Soc.* **1977**, *124*, 833.
(4) Kennedy, J. H.; Shinar, R.; Ziegler, J. P. *J. Electrochem. Soc.* **1980**, *127*, 2307.

0002-7863/87/1509-3581$01.50/0

an attractive feature for a practical photochemical reaction scheme. Mott–Schottky measurements place the bottom of the conduction band slightly above[16,17] or below[2,18] the H^+/H_2 half-cell potential, indicating thermodynamic feasibility, if not much driving potential, for water photodissociation without the application of external potential. One of the most interesting features of the photoconducting and photochemical behavior of iron oxide is its great sensitivity to sample preparation. The iron oxide phase diagram is complex and the compounds FeO and Fe_3O_4 exist with wide variation of stoichiometry. Clearly, the control of the solid state and surface chemistry of this compound is important in the understanding and optimization of its photochemical or catalytic properties.

After reporting that Mg-doped iron oxide coupled with Si-doped iron oxide in a p–n assembly, if illuminated with light of energy larger than 2.2 eV, produces hydrogen and oxygen without the application of an external potential[6], much work was carried out with this material. In a series of studies by Nakanishi et al.,[12] the photodissociation of water was monitored as a function of the atom fraction of the Mg-induced spinel phase in the α-Fe_2O_3 corundum polycrystalline sample. These samples were used as powders and were illuminated when suspended in an aqueous methanol solution. Maximum rates of H_2 evolution were found at about 35 atom % spinel phase inclusion. The results indicated that for these Mg-doped samples (a) the α-Fe_2O_3 semiconductor phase is essential for photochemical activity, (b) the photoproduction of H_2 can be optimized by the presence of the spinel phase, and (c) iron oxide suspensions as well as polycrystalline discs can be employed for the photoassisted production of hydrogen.

In this paper we report on the preparation and photochemical behavior of an iron oxide catalyst with much improved activity. This compound is undoped and produces hydrogen when illuminated with light of band gap or larger energy at 20 times higher rates than the Mg-doped iron oxide previously reported. As a result of this higher activity we could determine conclusively that the photoproduction of H_2 from water is catalytic. The iron oxide catalysts can be prepared and utilized both as powders and polycrystalline pellets.

Experimental Section

(A) Catalyst Preparation. Partially reduced ferric oxide was used in the form of powder and sintered pellets. The powder form can be prepared by exposing α-Fe_2O_3 (Baker AR 99.95%) for 8 h at 450 °C to a flowing mixture of 70 vol % H_2 (99.99%) and 30 vol % H_2O vapor at 1 atm and then heating in O_2 (99.5%) or air at 450 °C for 10 min.

One-half inch diameter pellets of iron oxide were prepared by pressing 500 mg of α-Fe_2O_3 powder at 7000 kg/cm^2. The pressed pellets were then sintered at 1150 °C for 20 h. The sintered pellets could be activated by reacting first with 70 vol % H_2–30 vol % H_2O at 500 °C and 1 atm for 10 min and then with O_2 at 450 °C for 10 min.

In order to avoid fracture of the pellets during the reduction step, an alternative reduction was performed. This consists of treating the sintered pellets at 500 °C for 1.5 h in a mixture of 4 vol % H_2–46 vol % Ar and 50 vol % H_2O at 1 atm. This reduction step was also followed by reoxidation as indicated above.

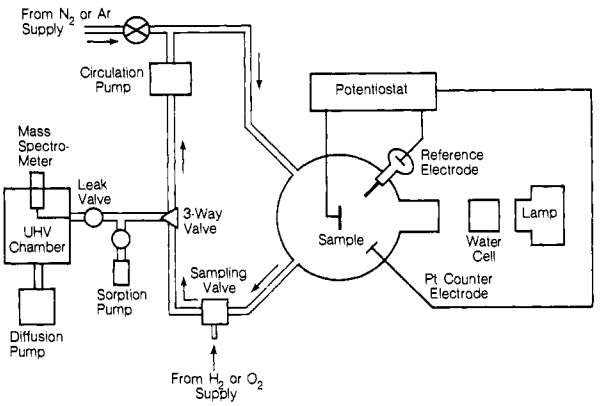

Figure 1. Apparatus for simultaneous studies of photocurrents and photoelectrochemical production of H_2 and O_2. For photocatalytic hydrogen production studies, a similar arrangement was used without electrodes.

(B) Catalyst Characterization. (1) X-ray Diffraction. Powder diffraction patterns of the catalyst were taken by a Siemens Model D500 powder diffractometer equipped with a Cu $K\alpha_1$ monochromated light source (λ = 1.5405 Å). The diffraction patterns were taken in the region of 2θ between 15° and 65°. For qualitative analysis the 2θ scan rate was 6 deg/min, and for quantitative analysis a slower scan rate was used (1 deg/min). The diffraction pattern was the superposition of the corundum and spinel lines of the iron oxides. The composition of the catalyst was estimated by comparing the ratio of the integrated intensity of the 220 spinel and the 012 corundum reflections with known standards consisting of mixtures of Fe_3O_4 (Alfa products 99.95%) and α-Fe_2O_3. The composition was also checked by Mössbauer spectroscopy with a ^{57}Co in Pd source in the constant acceleration mode.

(2) Chemical Analysis. Samples of the powdered catalyst were dissolved in 6 M HCl (Fisher Scientific) solution at room temperature. Ar gas was bubbled through the solution during the process. After complete dissolution, the concentration, of Fe(II) and Fe(III) were determined by titration against a standard solution of $KMnO_4$ (Mallinckrodt AR). Fe(II) was titrated directly against $KMnO_4$. To measure the total amount of iron, Fe(III) was first reduced by a $SnCl_2$ solution (Mallinckrodt AR) to Fe(II) and then titrated against $KMnO_4$.

(3) Photocurrents. The pellets were prepared for electrochemical measurements by making electrical contact between a wire and a pellet with silver epoxy (Tra-con, Bipex). The contact was sealed from the solution by using silicon rubber (Dow Corning, silastric 732 RTV). The electrochemical response of these electrodes was investigated as a function of the applied voltage both in the dark and under illumination. Potentiodynamic measurements of dc photocurrents were carried out in a three-compartment cell. An active pellet was serving as the working electrode, 1 cm^2 of platinum foil was used as the counter electrode, and a Saturated Calomel Electrode was used as the reference electrode. Illumination of the sample was performed by a 300-W halogen–tungsten lamp. Infrared radiation was suppressed by passing the light through a water filter. It was then focused on the samples by using quartz optics. Current–voltage curves were obtained by using a Pine RDE3 potentiostat.

(4) Flat Band Potential Determination. Impedance measurements for partially reduced ferric oxide electrodes in 0.1 M NaOH solution (Mallinckrodt AR) were performed at various frequencies (1 to 20 KHz). The flat band potential was determined from the corresponding Mott–Schottky plots.[19,20]

(C) Measurements of the Photochemical Production of Hydrogen and Oxygen. Two types of experiments were performed in this study. In one, the catalyst, either in powder or pellet form, was enclosed in a cell without any external electrical connection. We refer to these as the photocatalytic experiments.

Another type of experiments were aimed at establishing correlations between the photoproduction of hydrogen and the solid-state properties of our catalyst. In these experiments the samples were in the form of pellets and were used as a working electrode in a three-compartment electrochemical cell. A Pine RDE3 potentiostat was used in these experiments. We refer to these as photoelectrochemical experiments.

(1) Photocatalytic Production of Hydrogen. In order to investigate the catalytic formation of H_2, the experiment was carried out in a closed loop with 1 atm of N_2 circulating through a cell containing either a slurry of 30 mg of powdered catalyst or a pellet in 30 mL of deionized water.

(5) Sanchez, H. L.; Steinfink, H.; White, H. S. *J. Solid State Chem.* **1982**, *41*, 90.
(6) Leygraf, C.; Hendewerk, M.; Somorjai, G. A. *J. Catal.* **1982**, *78*, 341.
(7) Turner, J. E.; Hendewerk, M.; Parmeter, J.; Neiman, D.; Somorjai, G. A. *J. Electrochem. Soc.* **1984**, *131*, 1777.
(8) Sharon, M.; Prasad, B. M. *Sol. Energy Mater.* **1983**, *8*, 457.
(9) Itoh, K.; Bockris, J. O'M. *J. Electrochem. Soc.* **1984**, *131*, 1266.
(10) Sieber, K. D.; Sanchez, C.; Turner, J. E.; Somorjai, G. A. *J. Chem. Soc., Faraday Trans. 1* **1985**, *81*, 1263.
(11) Sanchez, C.; Hendewerk, M.; Sieber, K. D.; Somorjai, G. A. *J. Solid State Chem.* **1986**, *61*, 47.
(12) Nakanishi, H.; Sanchez, C.; Hendewerk, M.; Somorjai, G. A. *Mater. Res. Bull.* **1986**, *21*, 137.
(13) Lichtin, N. N.; Vijayakumar, K. M.; Khader, M. M. Proceedings of the June 1985 meeting of the International Solar Energy Society, Montreal, Montreal, Canada; E. Bilgen, K. G. T. Hollands, Eds.; p 433.
(14) Khader, M. M.; Lichtin, N. N.; Vurens, G. H.; Salmeron, M.; Somorjai, G. A. *Langmuir* **1987**, *3*, 303.
(15) Strenlow, W. H.; Cook, E. L. *J. Phys. Chem. Ref. Data* **1973**, *2*, 163.
(16) Kennedy, J. H.; Frese, K. W., Jr. *J. Electrochem. Soc.* **1978**, *125*, 723.
(17) Horowitz, G. C. *J. Electroanal. Chem.* **1983**, *159*, 421.
(18) Anderman, M.; Kennedy, J. H. *J. Electrochem. Soc.* **1984**, *131*, 21.
(19) Mott, N. F. *Proc. Roy. Soc. (London)* **1939**, *A171*, 27.
(20) Shottky, W. *Z. Phys.* **1939**, *113*, 367; **1942**, *118*, 539.

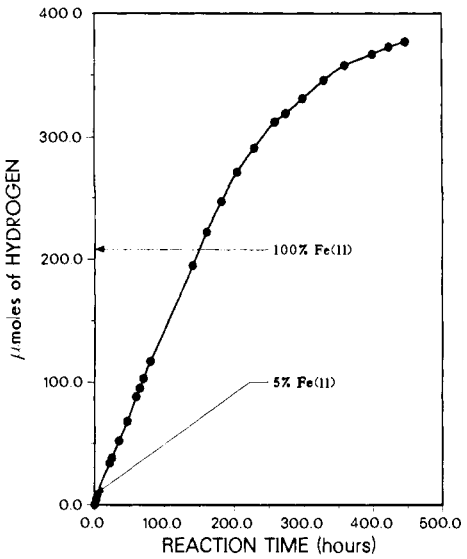

Figure 2. Cumulative hydrogen production from 30 mg of powder of a partially reduced Fe_2O_3 catalyst suspended in 30 mL of deionized water. The catalyst was illuminated with visible light of 20 mW/cm^2 intensity from a Xe lamp. The catalyst contains approximately 5 mol % of Fe_3O_4. For comparison the H_2 that would be formed by the oxidation of Fe(II) to Fe(III) in the sample is indicated by the arrows, for the case of 5% and 100% of Fe(II) in the sample.

This cell was illuminated by visible light from a 150-W Xe lamp. The light intensity was 20 mW/cm^2 over an illuminated cell area of 15 cm^2. The gas stream was periodically leaked into a UHV chamber, where it was analyzed with a quadrupole mass spectrometer. The mass spectrometer was calibrated for H_2 and O_2 as follows:

The reaction loop was filled first by the circulating gas (Ar or N_2), and then known volumes of H_2 or O_2 were added to the circulating gas by a sampling valve. After the gases were mixed inside the loop by a circulation pump, the gaseous mixture was leaked into the UHV chamber. In this manner, calibration curves were constructed by plotting the intensity of the mass 2 peak (in the case of H_2 calibration) or the intensity of the mass 32 peak (in the case of O_2 calibration) vs. the volume of gases (H_2 or O_2) added in the reaction loop.

To eliminate the possibility of spurious effects due to air leaks in O_2 detection, we used $H_2{}^{18}O$ water (Cambridge Isotope Labs, 20% concentration). The stoichiometry of H_2O splitting was then measured by comparing the signals at mass 34 and 36. We assumed random mixing of ^{16}O and ^{18}O in our calculation. We also assumed that the mass spectrometer sensitivity for $^{36}O_2$ and $^{34}O_2$ was identical with that for $^{32}O_2$. A schematic of the reaction loop and mass spectrometer detector is shown in Figure 1.

(2) Photoelectrochemical Production of H_2. Photoelectrolysis of water was performed in the electrochemical cell. The working electrode was a pellet of the partially reduced ferric oxide, and the counter electrode was a platinum foil with a SCE reference electrode.

The wavelength dependence of the photocurrents and H_2 production was investigated by filtering the light with a series of color filters (Corning Color Filters) and renormalizing the results to the total light intensity as measured with a calibrated EPPLY thermopile.

Results

(A) Photocatalytic Experiments. (1) H_2 Production. The Fe_2O_3 catalyst that was used in this study contained 3–5 mol % of Fe(II) as was determined by chemical analysis. X-ray diffraction showed that a spinel phase exists in amounts of less than 10 mol %. Mössbauer spectroscopy revealed that the catalyst consists of a mixture of Fe_2O_3 and Fe_3O_4. From the areas of the peaks we determined that Fe_3O_4 is present in amounts of approximately 5 mol %.

Figure 2 shows the accumulation of H_2 as a function of time over the iron oxide catalyst slurry. At a constant light intensity with visible light, H_2 production can be sustained for over 400 h. This amounts to 380 μmol of H_2 while the total number of moles of Fe_2O_3 is 190 μmol. Assuming that all the catalyst particles were active during the experiment, the rate of H_2 generation is 40 μmol h^{-1} g^{-1} for the first 200 h. BET measurements indicate an area of 1.85 m^2/g for the fresh active catalyst.

A blank experiment (no catalyst was used) and a dark experiment were performed, each for 24 h. The amount of H_2 detected was less than the detection limit of the mass spectrometer (2 μmol). This means that the dark electrolysis of H_2O, if there is any, would not contribute to the H_2 production by more than 10%.

If we make the assumption that the surface area remains constant during the experiments and that all of the surface atoms are active, we obtain a lower limit of the turnover rate of 10^{-4} molecules site^{-1} s^{-1}. This figure is likely to be largely underestimated on account of the larger catalyst area (550 cm^2) as compared to the illuminated area (15 cm^2).

Assuming that the catalyst contained 5 mol % Fe(II) (in the Fe_3O_4), the yield of H_2, obtained in 450 h, is equivalent to 80 times the stoichiometic reducing capacity of the catalyst according to the reaction

$$2Fe_3O_4 + H_2O \rightarrow 3Fe_2O_3 + H_2$$

In fact no significant consumption of Fe(II) was detected either by X-ray diffraction or by oxidimetric titration of samples of the used catalyst. If, for comparison, we assume that all Fe is initially Fe(II) and if it then oxidizes completely to Fe(III), the amount of measured H_2 would still be over twice the amount of iron in the catalyst as indicated in Figure 2 by the arrows. Thus we conclude that the photoproduction of H_2 from water is catalytic.

(2) O_2 Production. In a separate experiment $H_2{}^{18}O$ was used to study the stoichiometry of the reaction. The amount of O_2 detected was 40 ± 15% of the amount of hydrogen detected in the same experiment.

(B) Photoelectrochemical Experiments. (1) Light Intensity Dependence of Photocurrents and H_2 Production. When the samples were mounted on the electrochemical cell in the manner indicated in the Experimental Section, the photocurrent was found to increase linearly as shown in Figure 3A, from 10 μA to over 160 μA by varying the light intensity by about an order of magnitude. We measured also the rate of H_2 evolution as a function of light intensity as shown in Figure 3B. We find that under the conditions of +0.5 V bias the H_2 evolution is linearly increasing from 0 to 17 μmol in 10 h, with increasing light intensity. This figure implies a lower limit to the efficiency of light conversion to H_2 of 10^{-3} molecules per photon.

(2) Wavelength Dependence of Photocurrents and H_2 Production. The results of the measurements of photocurrents and H_2 production as a function of the light energy are presented in Figure 4, A and B, respectively. The working electrode was biased with +0.5 V vs. SCE in a 0.1 M NaOH solution. The photocurrent has a threshold at 2.1–2.3 eV and it reaches a constant high value at 3 eV at a given light intensity. Similarly the H_2 production has a threshold at about the same light energy and it reaches a constant value at 3 eV.

(3) Photocurrent and H_2 Production as a Function of Applied Voltage. Photocurrent, dark current, and H_2 production change as a function of the applied voltage as shown in Figure 5, parts A and B, respectively. If the hydrogen production is plotted vs. the photocurrent using the data from Figure 5A and B a linear relation between −0.1 and +0.7 V is observed as shown in Figure 6.

(4) Flat Band Potential Measurements. The pellets of the active catalyst were mounted in the three-electrode electrochemical cell, and its capacitance was measured as a function of applied bias. The Mott–Schottky plots obtained were all similar to that shown in Figure 7. The intercept of each curve with the abscissa varied from sample to sample, or within one sample as a function of time, depending on the value and duration of the negative bias applied above −0.7 V, where the cathodic reduction modifies the surface in a noticeable way. The flat band potentials determined in that manner varied between −0.9 and −1.1 V with respect to SCE at pH 13. The frequency used in the various experiments did not change the value of the intercept (between 1 and 20 kHz). However, the slope of the curves changed by an order of magnitude between these frequency limits, corresponding to a donor density between 10^{18} and 10^{19} cm^{-3}. Clearly, the simple capacitor model

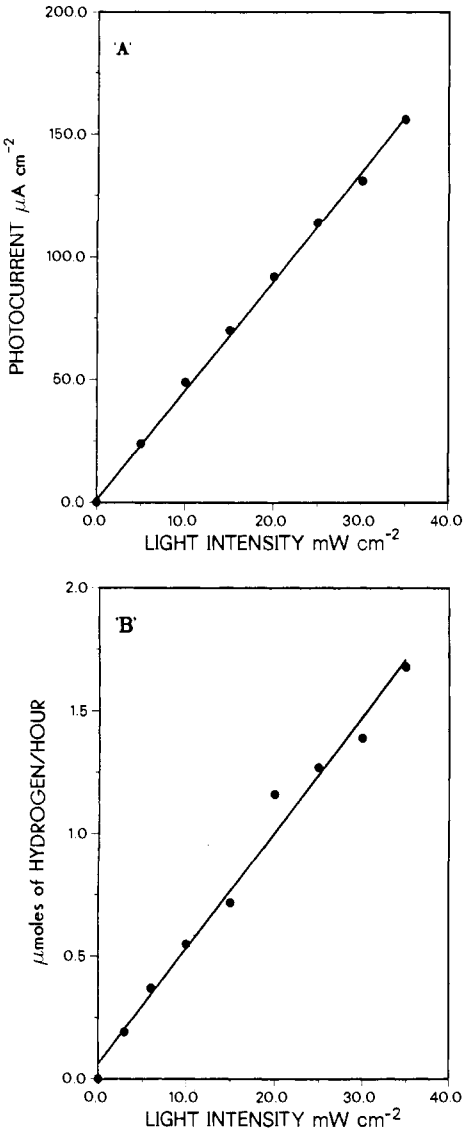

Figure 3. Photocurrent (A) and hydrogen production (B) vs. light intensity for a pellet of partially reduced Fe_2O_3. The pellet was biased at +0.5 V with respect to the SCE in a 0.1 M NaOH solution.

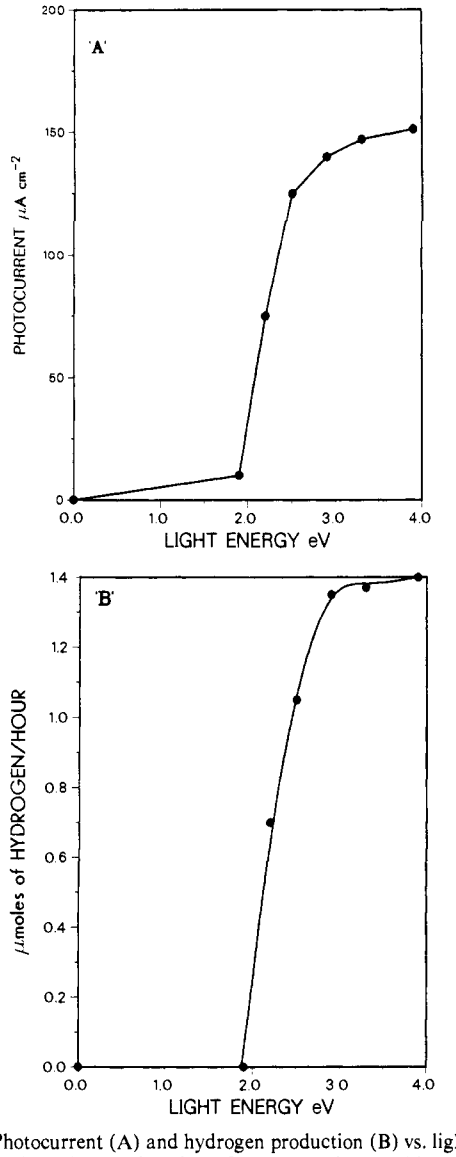

Figure 4. Photocurrent (A) and hydrogen production (B) vs. light energy for a pellet of partially reduced Fe_2O_3. The pellet was biased at +0.5 V with respect to the SCE in a 0.1 M NaOH solution.

of the semiconductor surface is not adequate to describe the behavior of the space charge region of an iron oxide catalyst.

Discussion

The iron oxide catalyst used in this study was over 20 times more active than the Mg-doped iron oxide that was used in previous studies[12] for the photodissociation of water to H_2 and O_2. As a consequence we could readily determine that the photodissociation process is catalytic. The best proof of catalytic behavior is that more H_2 is formed in the powder catalyst suspension than the total amount of iron in the catalyst. If only the surface atoms are catalytically active, then the figures mentioned in the results section largely overestimate the nubmer of iron atoms that may be active. Even within these strict limits the reaction has proven to be catalytic. Another indication of the catalytic character of the photodissociation of water is the fact that O_2 could be detected in amounts not far (40 ± 15%) from the expected stoichiometric ratio.

Let us now discuss the photoelectrochemical results. The hydrogen production is approximately 1 μmol per h at +0.5 V and pH 13. This is equal to about 2×10^{14} molecules/s. The photocurrents measured in this case were 200 μA. This corresponds to 1×10^{15} electron-hole pairs generated per second that reach the surface to perform oxidation and reduction reactions. Thus the efficiency appears to be approximately 0.2 H_2 molecules per electron-hole pair generated. Since the pellets are discs of 0.5 in. in diameter, we assume an area of 1.3 cm^2. So the 2×10^{14} molecules per second would give a turnover rate of 0.2 molecules per site per second assuming 1×10^{15} sites per cm^2.

It is clear from Figure 6 that the H_2 production increases linearly with the photocurrent over a large range of biases (−0.1 to +0.7 V). Above +0.7 V the H_2 production increases faster than the photocurrent because of the increasing dark current. As can be seen in that figure, H_2 evolution is observed even at zero photocurrent. This means that there is no net flow of charge across the circuit and therefore both electrons and holes are consumed at the working electrode.

We can attempt to explain the observed results within the solid state band model of the semiconductor–solution interface. In this model, electrons and holes are produced by the absorption of light of energy greater than the band gap of Fe_2O_3, which is 2.2 eV, in agreement with our observations. The observed linear relation between both photocurrent and H_2 production rate and light intensity support this type of model.

In order to explain the production of both H_2 and O_2 in the same particle or sample in our unbiased experiments we have to assume that both electrons and holes can reach the solid–solution interface to perform reduction and oxidation reactions. This presents several difficulties. First the Fe_2O_3 is an n-type semiconductor, indicating that its band bending in normal anodic operation is such that electrons are driven to the bulk, while holes are driven to the surface. In our electrically isolated catalyst,

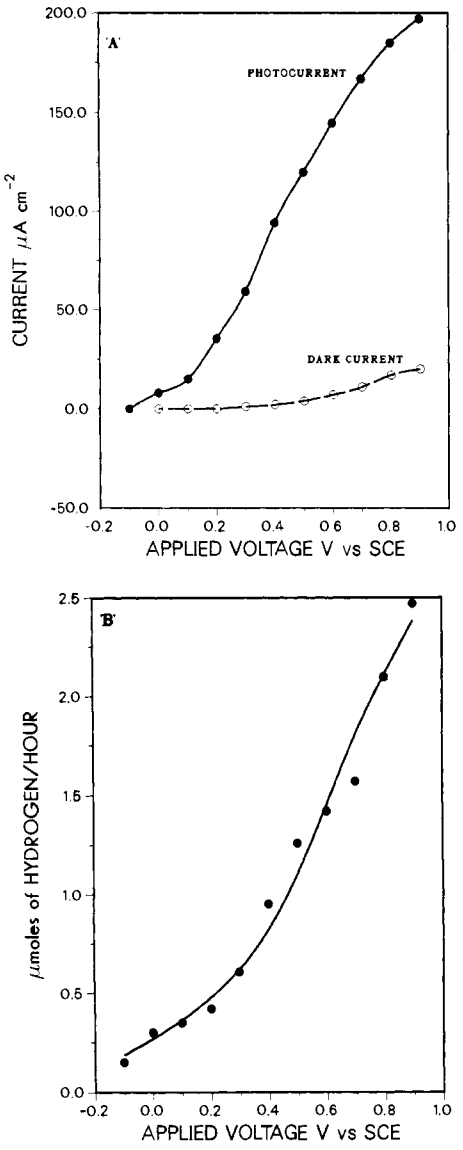

Figure 5. Photocurrent and dark current (A) and hydrogen production (B) vs. applied voltage for a pellet of partially reduced Fe_2O_3. The pellet was illuminated by visible light of intensity 30 mW/cm² in 0.1 M NaOH.

however, this process cannot be sustained as it would lead to negative charging of the particle. We are thus led to assume that in steady state a band bending is reached in such a way that either the bands are flat and all electrons and holes recombine or that the band bending changes with the position on the surface in a way that both can reach the surface at different locations. If this solid-state model is to account for the observed photoproduction of H_2 and O_2, it appears that the isolated particles have anodic and cathodic regions where the holes and electrons are transported and where oxidation and reduction reactions take place. This idea of a catalyst particle is not new in the context of metal covered oxide particles.[21,22]

We do not know at this stage whether the presence of Fe_3O_4, which is the result of catalyst preparation, is essential to the functioning of the catalyst or if it is only a byproduct of other modifications in the Fe_2O_3 crystal that are desirable for enhanced catalytic activity. These modifications might include the formation of more surface defects and lattice oxygen vacancies that might affect charge transport to the surface of Fe_2O_3. We also cannot exclude the formation of other phases of iron oxide e.g., γ-Fe_2O_3. We are presently performing X-ray and Mössbauer spectroscopy experiments with thin films of iron oxide to obtain more detailed information on the nature of the surface films ($\lesssim$1 000 to 10 000 Å).

(21) Aspnes, D. E.; Heller, A. *J. Phys. Chem.* **1983**, *87*, 4919.
(22) Gerischer, H. *J. Phys. Chem.* **1984**, *88*, 6096.

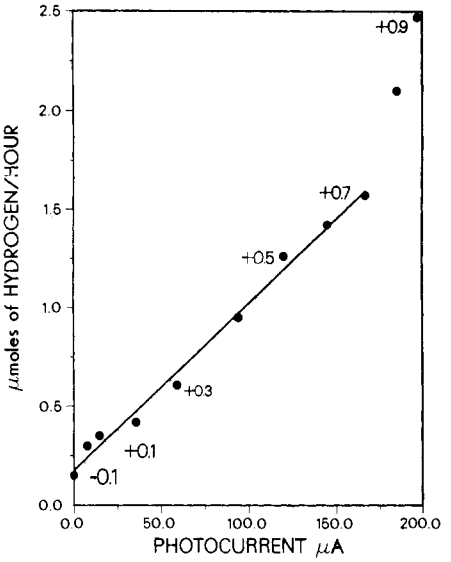

Figure 6. Hydrogen production as a function of the corresponding photocurrent obtained from the data in Figure 5, A and B. Each point corresponds to a different bias voltage.

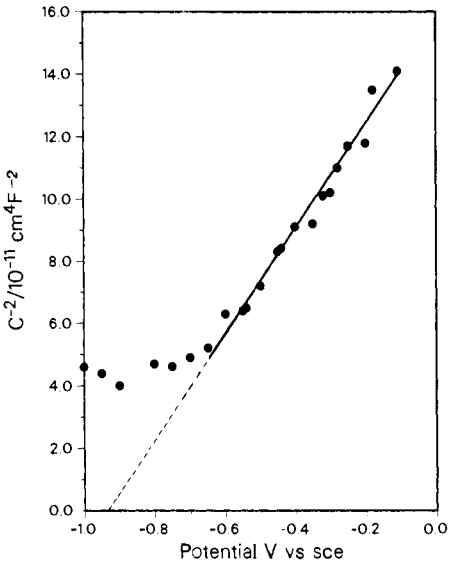

Figure 7. Mott–Schottky plot corresponding to an active iron oxide catalyst in pellet form. The modulation frequency is 1 kHz and the solution is 0.1 M NaOH. The deviation from the straight line above −0.7 V (vs. SCE) corresponds to the onset of the cathodic reduction of the sample.

Another point to be considered in the formation of H_2 and O_2 on the unbiased samples involves the exchange of oxygen from the water and the iron oxide lattice. The energy needed for the creation of oxygen vacancies in an oxide semiconductor is related to the value of the bandgap energy.[23] After the creation of a vacancy by energetic photons ($h\nu > 2$ eV), subsequent water adsorption and hydrogen desorption complete the oxygen exchange. Experiments are currently performed to study the possibility of exchange of ^{18}O from $H_2{}^{18}O$ with ^{16}O in the Fe_2O_3 lattice.

Acknowledgment. This work was supported by the Director, Office of Basic Energy Sciences, Chemical Science Division of the U.S. Department of Energy under Contract No. DE-AC03-76SF00098. One of the authors (M.M.K.) thanks the Egyptian Ministry of Education for the award of a fellowship.

Registry No. Fe_2O_3, 1309-37-1; Fe_3O_4, 1317-61-9; H_2, 1333-74-0; H_2O, 7732-18-5; O_2, 7782-44-7; $H_2{}^{18}O$, 14314-42-2; Fe^{2+}, 15438-31-0.

(23) Klissurski, D. G. *Solid State Commun.* **1974**, *15*, 1789.